# Novel Materials for Combined Nitrogen Dioxide and Formaldehyde Pollution Control under Ambient Conditions

**Hugo S. Russell** [1,2,3,4] **, James Bonomaully** [2] **, Rossana Bossi** [4] **, Magdalena E. G. Hofmann** [5] **, Hasse C. Knap** [2] **, Jakob B. Pernov** [1,4] **, Marten in 't Veld** [1] **and Matthew S. Johnson** [1,2,*]

[1] Department of Chemistry, University of Copenhagen, Universitetsparken 5, DK-2100 Copenhagen Ø, Denmark; hugo.russell@envs.au.dk (H.S.R.); jbp@envs.au.dk (J.B.P.); Marten.Veld@idaea.csic.es (M.i.V.)

[2] AirLabs Denmark, Nannasgade 28, DK-2200 København N, Denmark; james.bonomaully@airlabs.com (J.B.); hasse.knap@gmail.com (H.C.K.)

[3] Danish Big Data Centre for Environment and Health (BERTHA), Aarhus University, DK-4000 Roskilde, Denmark

[4] Department of Environmental Science, Aarhus University, Frederiksborgvej 399, DK-4000 Roskilde, Denmark; rbo@envs.au.dk

[5] Picarro B.V., Willemsplein 2, NL-5211 AK 's-Hertogenbosch, The Netherlands; mhofmann@picarro.com

[*] Correspondence: msj@chem.ku.dk; Tel.: +45-3532-0300

**Abstract:** Formaldehyde (HCHO) and nitrogen dioxide ($NO_2$) often co-exist in urban environments at levels that are hazardous to health. There is a demand for a solution to the problem of their combined removal. In this paper, we investigate catalysts, adsorbents and composites for their removal efficiency (RE) toward HCHO and $NO_2$, in the context of creating a pollution control device (PCD). Proton-transfer-reaction mass spectrometry and cavity ring-down spectrometry are used to measure HCHO, and chemiluminescence and absorbance-based monitors for $NO_2$. Commercially available and lab-synthesized materials are tested under relevant conditions. None of the commercial adsorbents are effective for HCHO removal, whereas two metal oxide-based catalysts are highly effective, with REs of 81 ± 4% and 82 ± 1%, an improvement on previous materials tested under similar conditions. The best performing material for combined removal is a novel composite consisting of a noble metal catalyst supported on a metal oxide, combined with a treated active carbon adsorbent. The composite is theorized to work synergistically to physisorb and oxidize HCHO and chemisorb $NO_2$. It has an HCHO RE of 72 ± 2% and an $NO_2$ RE of 96 ± 2%. This material has potential as the active component in PCDs used to reduce personal pollution exposure.

**Keywords:** pollution control; NOx; formaldehyde; activated carbon; composite filter; catalytic removal; adsorbent filter; indoor air quality; urban air quality

## 1. Introduction

Harmful levels of air pollution are a reality across the globe, and excess mortality due to all air pollutants is estimated at 8.8 million deaths per year [1,2]. Air pollution has many components in both the gas and particulate phase. Both formaldehyde (HCHO) and nitrogen dioxide ($NO_2$) are of specific concern and are linked with health impacts due to their elevated levels in indoor environments including homes, offices and cars. Products have been developed with the aim of removing these pollutants individually. However, while reasonable $NO_2$ control systems exist, only limited success has been achieved for HCHO removal, and a solution has not been found for the combined removal of $NO_2$ and HCHO.

### 1.1. Formaldehyde Emissions and Health Effects

HCHO is emitted in the indoor environment by building materials including engineered wood products, textiles, glues and polymers, as well as being produced in situ during cooking and by the reactions of ozone with terpenes in air [3–6]. It is commonly found at elevated levels in enclosed environments, including new and recently renovated, well-sealed buildings and cars, where emissions are high and air exchange may be low [7–11]. In these environments, HCHO can be found at levels greatly exceeding the World Health Organization (WHO) threshold limit of 0.1 mg m$^{-3}$ (~81 parts per billion (ppb)) [12]. HCHO is also increasingly becoming an issue in ambient (outdoor) air, meaning that exchange with outdoor air is not necessarily beneficial [13].

HCHO is associated with adverse health effects that range from sensory irritation and decreased pulmonary function to nasopharyngeal cancer, leukemia and lymphohematopoietic malignancies. Formaldehyde is classified as a group 1 carcinogen by the International Agency for Research on Cancer (IARC) [5,14–16]. It has been shown that both short-term, high concentration exposure and long-term, low concentration exposure to HCHO are harmful [5,17]. The combination of high concentration and high toxicity mean that, in China, for example, the cancer risk associated with HCHO is the greatest of all volatile organic compounds (VOCs), and therefore its effective control is a priority [12,17].

### 1.2. Nitrogen Dioxide Emissions and Health Effects

Nitrogen dioxide (NO$_2$) is typically an outdoor pollutant produced when air is heated—for example, in diesel engines and power plants [18,19]. However, in urban environments, it can also exist at high levels inside homes and vehicles due to indoor sources, such as cooking, as well as exchange with the outdoor air [20–24]. According to the WHO, it has been implicated in a host of direct, negative health effects including airway irritation, asthma, respiratory disorders and lung cancer, as well as having a powerful impact on the cycles involved in the production of other pollutants such as ozone and particulate matter (PM), which are both associated with further negative health outcomes [25,26].

### 1.3. Problems with the Current State-of-the-Art Pollution Control Methods

HCHO and NO$_2$ have been shown to exist as co-pollutants in enclosed environments that are suitable for the use of pollution control devices (PCDs) [21]. A range of different methods have been developed and tested for their removal; however, each presents different disadvantages and the issue remains unsolved, particularly in the case of HCHO, which is considered challenging to remove due to its high vapor pressure [27,28].

Under ambient conditions, it is expensive and inefficient to use control methods that require additional input of power or consumable liquid reactants, ruling out such methods as wet scrubbers, thermal catalysts, photolysis, selective catalytic reduction (SCR) or bio-filters [27,29]. Other possible control methods have also been shown to be ineffective or problematic, such as negative-ion cleaners and conventional physisorbents [28,30]. Phytoremediation and other biological remediation methods have been shown to have some effect on concentrations of HCHO but have still not been proven to maintain high enough removal over time to significantly lower concentrations [31]. They also require careful monitoring and control of environmental parameters to ensure the longevity of the biological system [32].

Some available air purifiers, such as those based on ozone, photo-catalysis or negative-ions, have even been shown to produce HCHO, amongst other by-products, and particle filters in heating, ventilation, and air conditioning (HVAC) systems have also been shown to release HCHO due to the glue used in their production [28,33,34].

The advantages and disadvantages of the different methods available for HCHO removal are summarized in a recent book chapter by Wang et al. [32] and a critical review by Pei and Zhang [28]. From these works, a clear direction forward is not identified, but non-thermal catalysis and chemisorption are identified as the best currently existing processes due to their potential for efficient

removal combined with low installation and maintenance costs [28]. However, existing adsorbents are regarded as lacking in efficiency and room temperature catalysts are regarded as too expensive for use at scale due to the noble metals used in their production [30]. A recent review of the state of the art in sorbents for formaldehyde by Na et al. [30] demonstrated some high performing novel adsorbents, such as metal organic frameworks and silylated graphite oxide, which show promise but are not yet produced at the scale needed for use in commercial products. The article also suffered from a lack of standardized testing, meaning that the materials are difficult to compare and overall capacity and partition coefficients were used; in their conclusion, they call for future studies to be conducted under conditions more relevant to actual use [30].

Conversely, there has been more success with $NO_2$ removal efforts. Chemisorption of $NO_2$ onto treated active carbon (AC) and other porous adsorbents has been shown to be an effective method for ambient $NO_2$ removal [35]. However, as described above, no technology has emerged for the effective removal of HCHO under these conditions and, in particular, no solution exists for the combined removal of both HCHO and $NO_2$. This is in part due to the two gasses having very different chemical and physical properties [28].

*1.4. Scope of This Article*

In this project, a range of recently developed commercial and lab-synthesized materials were screened for their ability to remove HCHO. For those that are effective for HCHO, their ability to remove $NO_2$ in isolation was tested and, finally, their performance for a mix of the two pollutants. The range of materials tested included plain AC, chemically treated AC, graphite oxide, composite materials and various noble metal and metal oxide catalysts. The commercially available materials and lab-synthesized materials are compared under the same conditions, which are also directly relevant to ambient use.

As mentioned above, catalysts for HCHO removal are typically expensive due to the use of noble metals. In this study, a new approach is investigated that involves combining a physisorbent with a relatively small amount of catalyst with the aim of forming a synergistic mix, achieving effective HCHO removal with the minimum amount of catalyst and so having the potential to be used directly in a PCD.

## 2. Results and Discussion

*2.1. HCHO Removal*

Prior to the quantitative tests, an initial removal efficiency (RE) screening was performed in the chamber and single-pass setups for all of the materials described above. It was found that the graphite oxide (GO) had a negligible RE in the single-pass system (<10%, shown in Figure S5). This sample was uncharacterized, but, in the literature, it is seen to have pores with an average diameter in the mesopore region, which may be too large for effective physisorption of HCHO, as well as a low surface area and minimal functional groups [36]. Of the amine impregnated AC (IAC_2, IAC_3 and IAC_4), IAC_2 displayed a significantly shorter HCHO removal time in the chamber tests than plain AC, whereas IAC_3 and IAC_4 did not improve upon the plain AC (see Figure S6). IAC_3 is formed through the impregnation of AC with dimethylamine (DMA). This molecule does not undergo a reaction with HCHO to form imines, as described in Rong et al., as it is not a primary amine, which could explain its poor performance [37]. IAC_4 was synthesized by evaporating hexamethylene diamine (HMDA) onto AC, as described by Ma et al., where it is characterized as an HCHO adsorbent [38]. In their paper, it was tested under low flow and relatively high concentrations (1.5 L min$^{-1}$ and 2.2 ppm), which are not relevant for use in a PCD, which may explain its lower performance in this study. Due to their poor performance, IAC_3 and IAC_4 were deselected at the screening stage. The remaining materials were all selected for further HCHO removal testing.

The proton-transfer-reaction mass spectrometer (PTR-MS) was used for the initial screening and some subsequent tests. This technique can accurately measure HCHO at ppb levels in real time; however when a PTR-MS is used to measure species with a proton affinity similar to water, such as HCHO, the measured response is affected strongly by humidity [39,40]. This means that the absolute values obtained must be calibrated for varying humidity levels, which introduces additional error, particularly for chamber experiments where humidity may vary during the test period. The cavity ring-down spectrometer (CRDS) has similar performance to the PTR-MS but without crosstalk from variations in humidity and so was favored for the final quantitative tests (see supplementary material section: Uncertainty Determination and Instrument Comparison for further discussion).

HCHO breakthrough plotted against exposure is shown in Figure 1, with corresponding conditions shown in Table S1. The figures' X axis displays the cumulative exposure of the material to HCHO, which depends on the length of exposure and HCHO concentration; the Y axis displays the RE of the material and therefore the figure displays the effect of increasing exposure on RE. The level of exposure in the plot (up to 50 $\mu g\ cm^{-3}$) is equivalent to ~ 30 min of continual use in a PCD at an inlet HCHO mixing ratio of 80 ppb, assuming an air flow of 35 $m^3\ h^{-1}$ in the PCD. Therefore, a significant fall in RE during the test period would discount an adsorbent material for use in a PCD.
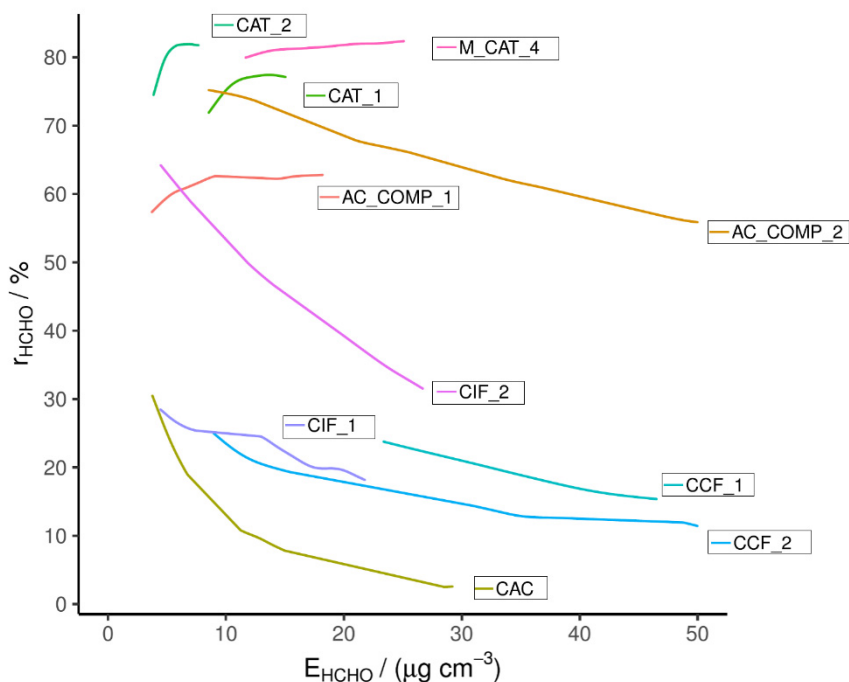


**Figure 1.** Single-pass HCHO removal efficiency measured with the PTR-MS.

### 2.1.1. Adsorbents

All of the commercially available active carbon-based adsorbents tested here (CCF_1, CCF_2, CIF_1, CIF_2 and CAC) display a low initial RE, as well as a rapid RE decrease over the testing period, with REs ranging from 3 to 32% at the end of the period (Figure 1). (A minor exception to this behavior is CIF_2, which exceeds this pattern by having a high initial RE). The most rapid fall in RE corresponds to the untreated AC (sample CAC). This is due to the high volatility of HCHO and the primarily non-polar surface of untreated AC [28,37]. A higher initial RE is seen for the commercial adsorbents, particularly CIF_2; however, their RE quickly drops with increasing exposure. These adsorbents were found to have a basic pH and have been shown to have a high RE for $NO_2$. Therefore it is assumed that they have been treated with basic agents known to improve the $NO_2$ removal of active carbon, such as KOH or $K_2CO_3$ [41,42]. This impregnation may slow the fall in RE through stronger interactions between the hetero-atoms introduced and the HCHO. Alternatively, the surface groups may result in

a less hydrophobic surface and therefore a larger water layer which allows HCHO dissolution from the gas phase; the Henry's law partitioning of HCHO is assisted by the equilibrium between aqueous formaldehyde and methane diol. The results suggest that these materials have not been optimized for HCHO removal and their limited interaction with HCHO means that their capacity is quickly exhausted [28]. The results of these commercial adsorbent tests show that the selected car cabin filters (CCF_1, CCF_2) and indoor filters (CIF_1, CIF_2) from market leading suppliers will not remove HCHO from enclosed environments effectively; the results also highlight the importance of producing a filter for this purpose. The data for adsorbent IAC_2 were omitted due to a test error; however, it was measured again in later rounds of testing (see Figure 2).
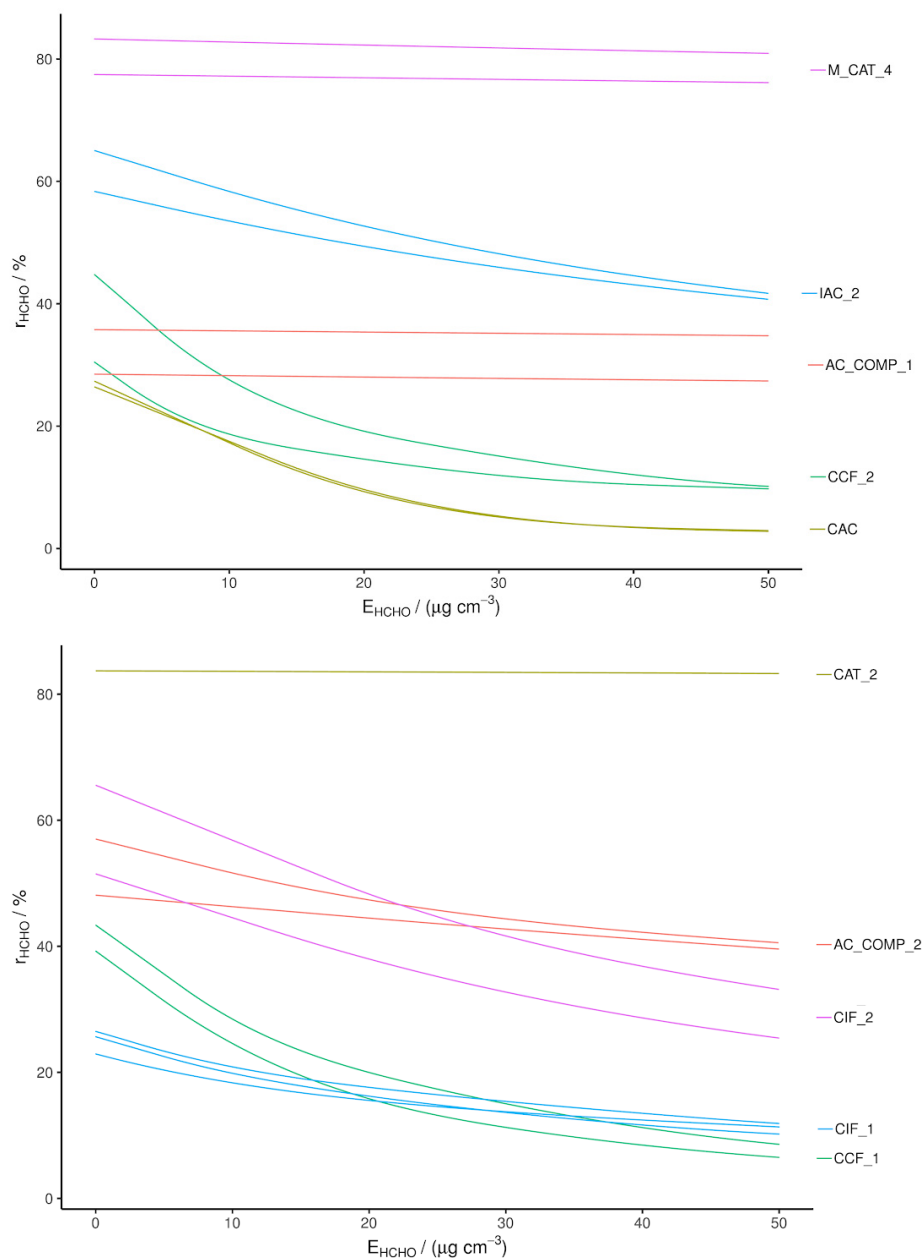


**Figure 2.** Single-pass HCHO removal efficiency measured with a CRDS, separated into two plots for ease of viewing.

### 2.1.2. Catalysts

Superior performance was seen for the catalysts (CAT_1, CAT_2 and M_CAT_4), which all displayed a RE above 60% during the test period.

CAT_1 and CAT_2 are examples of noble metal doped, metal oxide catalysts consisting of gold nanoclusters supported on $CeO_2$ and $TiO_2$, respectively. Both were effective for HCHO removal, with CAT_2 having a slightly greater RE of $82 \pm 1\%$ (at $7 \, \mu g \, cm^{-3}$) compared to $78 \pm 1\%$ (at $15 \, \mu g \, cm^{-3}$) for CAT_1. The mechanism of action for this type of catalyst has been discussed at length in the literature [28,43,44]. However, typically, $CeO_2$ supported Au nanocluster catalysts outperform those supported on other oxides such as $TiO_2$ [45,46]. This is not the case here, with a greater RE for the $TiO_2$ supported CAT_2. The Au content is quoted as being the same for both materials (~1%) and the specific surface area was found to be greater for CAT_1 (123.3 vs. $56.1 \, m^2 \, g^{-1}$). This type of catalyst has been shown to be strongly affected by the mixing and distribution of nanoparticles on the support; variation in this may explain the difference in RE recorded. The results of these tests compare favorably to previously reported catalyst examples, where elevated temperatures (40–360 °C) are required to reach REs of >80% and higher Au contents are used (minimum 2.5%) [45,46]. However, it is noted in review articles that direct comparison of this type of experimental data is difficult due to the variation in experimental setup and conditions employed [47].

M_CAT_4 is a $MnO_2$-based catalyst, with added KOH and $K_2CO_3$, but its exact composition is not known. Similar $Mn_xO_y$ catalysts have again been reported previously, composed from both pure $MnO_2$ and $MnO_2$ supporting noble metals or doped with other species [28,48–50]. They are purported to operate through the Mars and Van Krevelen (MVK) mechanism. This is an oxidative-reductive process and involves the interaction of a VOC with a site on the catalyst that has been oxidized by splitting molecular oxygen; the VOC then reacts with the oxygen, reducing the catalyst surface in the process; the surface oxygen is then replenished by reaction with molecular oxygen [28,51–53].

As mentioned above, direct comparison of filter RE is not trivial. For instance, in a study similar to the current one, single-pass HCHO removal by manganese oxide-based catalysts was tested. The authors reported a similar single-pass removal efficiency (77%) under ambient conditions. In this case, it was found that the addition of iron oxide ($Fe_2O_3$) increased the activity of $Mn_3O_4$ [54]. However, in another study, plain $MnO_2$ was reported to have an 80% conversion efficiency under ambient conditions in an HVAC system (although testing at half the face velocity), which is far higher than reported in the previously cited examples. On balance, the catalyst tested in this study seems to compare favorably to those previously reported in the literature, particularly for room temperature catalysis [48].

### 2.1.3. Composites

The two composite materials were found to have RE levels that would make them acceptable for use in a PCD.

AC_COMP_1 has the form of active carbon pellets. Due to the RE behavior characterized here and energy-dispersive X-ray spectroscopy (EDXS) analysis, it is thought to be a catalyst supported on AC [28,47,55]. This type of material has been reported in the literature with various metals and metal oxides supported on AC. According to EDXS analysis, AC_COMP_1 contains a number of elements besides carbon and, in fact, the surface images only show ~70% carbon by weight. Some of these elements have been observed in previous EDXS analyses of untreated pelletized carbon, including Mg, Al, Si, Ca, K and Fe. These are most likely due to impurities in the feedstock carbonaceous material. Other than these elements, the AC_COMP_1 surface also contains Cl, S, P and Na, which are not present in the untreated pelletized carbon, as well as a relatively large percentage of Fe (see Figure S7 for full analysis). These additional elements may be introduced due to the use of dehydrating salts, such as $MgCl_2$ and $CaCl_2$, which are commonly added to source materials prior to activation [56].

The efficient HCHO removal would suggest that this mix is produced by design and its removal behavior suggests that it is active catalytically. In particular, the presence of oxygen and various metals

suggest that a metal oxide supported on the AC could be acting to oxidize the HCHO. This has been shown in a number of studies but with recognized noble metal or metal oxide catalysts such as Ag nanoparticles or $MnO_2$ [28,55]. This mix of materials, or its components, does not correspond to the materials found in literature studies describing HCHO oxidation. Neither do the materials we found here correspond to AC-based chemisorbents described in the literature [28]. In one study, Fe doped graphene was shown to interact strongly with HCHO and trap it electrostatically but not oxidize it catalytically [57].

The material AC_COMP_2 showed a high initial RE (75%) but this was seen to decay during the experiment, dropping to 56% at 50 μg cm$^{-3}$ exposure. However, due to the nature of the composite material, which employs both physisorption and catalytic removal methods, this decay is expected to slow with increased exposure and to at least partially reverse during subsequent non-continuous periods of exposure. HCHO is theorized to physisorb onto the AC surface and then be gradually released to the catalyst at a level at which it can efficiently remove. This means that a filter that efficiently treats spikes in pollution concentration for large volumes of air can be produced using a minimal amount of costly noble metal catalyst. The contribution from the physisorbent is less during continual exposure as it becomes saturated but the system works to spread out peaks and the capacity is renewed by exposure to a flow of cleaner air.

## 2.2. Repeat HCHO Removal Tests

The initial tests conducted with the PTR-MS were repeated with the Picarro CRDS instrument to ensure their validity. For the loose materials, smaller quantities were used (0.4 g) to give an increased spread of results for the materials with larger Res; however, reducing the size of the test sample also increases the effect of material packing on the recorded results. The results of these tests are separated into two panels in Figure 2 for ease of viewing. The data from repeated tests are plotted to show the variation and the experimental conditions are detailed in Tables S2 and S3.

The CRDS results confirm the PTR-MS results, with rapid decay in RE from the adsorbents compared to no significant decay in RE from the catalysts. AC_COMP_1 also shows no significant decay in RE and the decay of RE for AC_COMP_2 has a different shape to that of adsorbent materials. IAC_2 displays a greater RE than the other adsorbents, demonstrating that treatment with primary amine groups is somewhat effective but still decays significantly during the test period, denoting a low capacity [37]. This is due to the saturation of amine sites at the carbon surface. In the literature, a large capacity (up to 447.8 mg g$^{-1}$) has been recorded, whereas, in our tests, its removal is seen to decay rapidly within 50 μg cm$^{-3}$ exposure [37]. The reason for this discrepancy may be due to the static adsorption technique used in the literature, as opposed to single-pass and chamber removal tests used here, and/or may be due to the AC substrate. In the literature, an activated Rayon fiber is impregnated with PABA; this type of AC is shown to have a very high oxygen content, up to 20%, whereas CAC beads have an oxygen content below 2%. It has been suggested that HCHO adsorption on AC occurs not only through the interaction between amine groups and HCHO but also due to cooperative action through hydrogen bonding to adjacent functional groups [28,37]. Rayon fibers have an increased coverage of these functional groups. In order to improve the capacity of IAC_2, an alternative AC substrate or pre-oxidation of the AC may be effective.

The relative REs and overall ranking of the materials when recorded with the CRDS instrument match with the PTR-MS results and therefore these results validate the PTR-MS tests. However, the original CAT_1 and CAT_2 samples gave lower recorded REs relative to those measured with PTR-MS. This may be due to ageing, as a new sample of CAT_2 was obtained which performed at least as well in the CRDS as the PTR-MS tests (shown in Figure 2).

Overall, the highest performing HCHO removal materials were CAT_2 and M_CAT_4. The composite materials also displayed sufficient removal capacity to be considered for further testing.

### 2.3. NO₂ Removal

The materials that showed promise in the HCHO tests were selected for $NO_2$ removal testing. This involved single-pass tests of the materials at 180–210 ppb $NO_2$; the results are shown in Figure 3, with test conditions in Table S4. In the table, RE is quoted for exposure at 300 $\mu g\ cm^{-3}$. This exposure represents less than one hour of continual use in a PCD at an inlet concentration of 150 ppb and an air flow of 35 $m^3\ h^{-1}$ in the PCD. Therefore, significant decay in RE during this period would discount a material for future use.
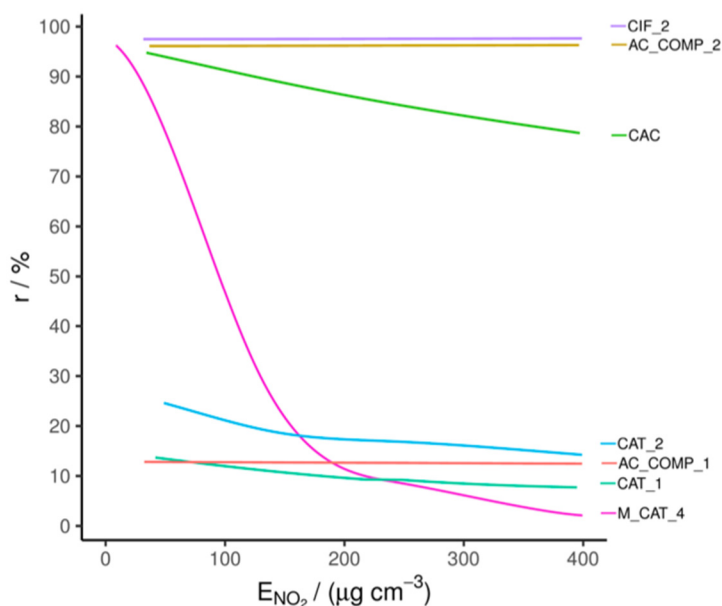


**Figure 3.** Single-pass $NO_2$ removal efficiency comparison.

#### 2.3.1. Adsorbents

The CIF_2 material, designed specifically for $NO_2$ adsorption, displayed a high RE, above 97%, that did not decrease during the testing period due to its surface treatment. In contrast, the untreated AC (CAC) has a similar initial RE, but this quickly falls during the test. This can be attributed to it having comparatively fewer active sites for adsorption and poorer transport through its pore structure, despite a marginally larger specific surface area (see Table S7) [35].

#### 2.3.2. Composites

The sample AC_COMP_1 is in pellet form, with an intermediate specific surface area of $488.3\ m^2\ g^{-1}$ and an average pore diameter of 3.6 nm (measured as described in Section 3.2). Based on these physical characteristics, and without an $NO_2$ specific treatment, a breakthrough curve similar to CAC would be expected; however, AC_COMP_1 has a relatively low RE for $NO_2$. This may be because surface treatments designed to improve HCHO adsorption may strip away groups involved in $NO_2$ chemisorption—specifically, surface-bound oxygen groups—and/or block micropores. The average pore size of 3.6 nm is larger than the previously noted optimum for $NO_2$ adsorption, which is in the micropore region (<2 nm diameter) [35]. However, $NO_2$ removal by AC_COMP_1 remains constant over the duration of the test, indicating either a catalytic mechanism or a large capacity, despite low efficiency. Conversely, AC_COMP_2 has a high RE (96 ± 2%) that does not decrease over the duration of the test. Based on the structure and our measurements, we surmise that this is because the treated AC in the composite effectively chemisorbs the $NO_2$.

### 2.3.3. Catalysts

Of the catalysts which were effective for HCHO removal (CAT_1, CAT_2 and M_CAT_4), none showed $NO_2$ removal of greater than 20% after 300 µg cm$^{-3}$ of exposure, demonstrating that they are relatively ineffective in this function. M_CAT_4 does show high initial $NO_2$ removal; however, this is likely due to the formation of a weakly physisorbed $NO_2$ layer which quickly saturates the relatively low number of available sites. The quick decay towards zero removal indicates that catalytic activity is effectively absent.

The established $NO_2$ adsorbent, CIF_2, and the composite AC_COMP_2 were the only materials that did not show a significant fall in RE and/or a low initial RE during the testing period; of these, only the AC_COMP_2 displayed a high enough HCHO removal in previous tests to be considered for use in a PCD.

### 2.4. Combined $NO_2$ and HCHO Removal

It is clear from the individual pollutant tests that only material AC_COMP_2 displayed sufficient removal of both $NO_2$ and HCHO individually to be considered a good candidate for use in a PCD. Therefore, it was tested for $NO_2$ and HCHO removal in a chamber with individual and combined exposure tests to ensure that the co-pollutants did not interfere with the removal of each other.

This type of testing is the most relevant to cleaning of small enclosed spaces such as car cabins, where pollution levels may begin relatively high but will quickly fall once the PCD is activated, as the rate of pollutant introduction is relatively slow. This environment favors the synergistic mix in AC_COMP_2 as the physisorption of the AC will smooth out the pollution peaks and allow the small amount of catalyst to remove it. After a period of time, at low pollutant concentration, the material will have desorbed and oxidized the HCHO and be ready for another peak.

The first-order rate constant $k$ values for the fitted decay curves from these tests are shown in Figure 4, with an example of the raw data in Figure S6, and the test conditions are displayed in Table S5. As can be seen from Figure 4, the removal rate for $NO_2$ was approximately twice that of HCHO but the speed of $NO_2$ and HCHO removal was not significantly different for individual vs. co-exposure.
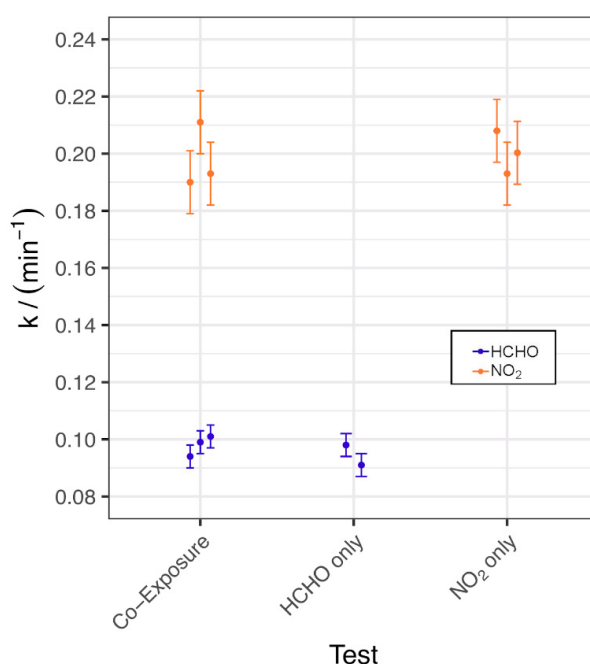


**Figure 4.** Calculated $k$ values for chamber removal tests of AC_COMP_2 under individual and co-exposure.

## 3. Materials and Methods.

### 3.1. Materials

A range of commercial and non-commercial materials was tested, described in Table 1. Untreated AC has been shown to be ineffective for removing HCHO, as expected for a material with a primarily non-polar surface [28]. A sample of untreated commercial AC (CAC) was included in these tests as a baseline material and to identify improvements in its performance from a number of chemical treatments. All of the chemically treated AC was derived from the same batch of CAC beads. The beads are spherically shaped activated carbon particles made from petroleum pitch by Kureha Corporation, in the size range 0.6 ± 0.05 mm. Untreated graphite oxide (GO) was also tested to determine whether it would be a suitable candidate for applying treatments to form an effective HCHO filter [58].

**Table 1.** Materials tested.

| Abbreviated Name | Material Description | Form | Synthesis Method/Company |
|---|---|---|---|
| CAC | AC beads | AC bead | Kureha Inc. |
| IAC_2 | CAC beads treated with para-aminobenzoic acid | AC bead | *Rong, Liu, Wu, Pan and Zheng, 2010* |
| IAC_3 | CAC treated with dimethylamine | AC bead | *Deliyanni and Bandosz, 2011* |
| IAC_4 | CAC treated with hexamethylene diamine | AC bead | *Ma, Li and Zhu, 2011* |
| CCF_1 | Treated AC granules mounted on a High-efficiency particulate air (HEPA) style filter | Mounted AC granules | Mann + Hummel GbH |
| CCF_2 | Treated AC granules mounted on a HEPA style filter | Mounted AC granules | Mann + Hummel GbH |
| AC_COMP_1 | Treated AC pellets | AC composite pellets | Xaiomi |
| AC_COMP_2 | Primarily AC-based composite material | AC composite beads | Airlabs |
| CIF_1 | Treated AC beads mounted on to polymer foam | Mounted AC bead | Purafil Inc. |
| CIF_2 | Treated AC beads | AC bead | Airlabs |
| M_CAT_4 | Metal oxide catalyst based on $MnO_2$ | Mounted Catalyst Powder | BASF SE |
| CAT_1 | Gold nanoparticle catalyst with a $TiO_2$ support | Rounded grains | Astrea Materials |
| CAT_2 | Gold nanoparticle catalyst with a $CeO_2$ support | Cylindrical grains | Astrea Materials |
| GO | Graphite oxide | Flakes | *Hummers and Offeman, 1958* |

Chemical treatments of AC have been shown to increase its ability to trap HCHO, typically through the addition of amine groups for chemisorption or noble metal nanoclusters that catalytically oxidize HCHO to $CO_2$ and $H_2O$ [37,55,59]. The addition of amine groups has also been shown to improve uptake of $NO_2$ onto AC and other porous adsorbents in separate studies [60,61]. In this study, the baseline CAC was treated with three specific amines to form samples IAC_2, IAC_3 and IAC_4.

IAC_2 is prepared by impregnating CAC with para-aminobenzoic acid (PABA), according to the synthesis described by Rong et al. [37]. Sample IAC_3 consists of AC beads impregnated with dimethylamine (DMA), as described by Deliyanni and Bandosz [60]. IAC_4 was formed through impregnation of HMDA onto the CAC beads via the procedure described by Ma et al. [38].

Commercial AC-based filter materials were selected to determine whether current market leading indoor air filters could effectively remove HCHO; these materials are marketed as being able to remove $NO_2$ effectively. The two car cabin filters (CCF_1 and CCF_2) in the test (sourced from Mann+Hummel GmbH) contain AC granules, whereas the two indoor filters (CIF_1 and CIF_2) utilize AC beads. CIF_1 is manufactured by Purafil Inc. and CIF_2 by Airlabs. The exact surface treatment of these materials is not disclosed.

Three commercial HCHO catalysts, all released in 2018, were also tested. These included a catalyst based primarily on $MnO_2$, which has previously been reported in the literature, but, in this case, with added KCl and $K_2CO_3$, designed to specifically target HCHO (M_CAT_4) [28,48,54]. BASF SE manufactures M_CAT_4 on a support (60 pores per inch (ppi) polymer foam). Two supported noble metal catalysts were also tested. These materials are designed primarily for the oxidation of CO and other VOCs but are quoted as being able to remove HCHO and reactive nitrogen oxides. Both of these catalysts are based on gold nanoparticles, one with a $CeO_2$ support substrate (CAT_1) and the other a $TiO_2$ support (CAT_2). Similar catalysts appear in the literature [28,43,45,46]. Astrea Materials SI manufactures the samples tested here.

The sample AC_COMP_1 is an active carbon-based composite, containing a range of chemical elements on the surface of active carbon pellets; EDXS analysis of this is shown in Figure S7, where it appears to act catalytically in the removal of HCHO.

AC_COMP_2 is also a composite material based on treated AC and a metal oxide supported noble metal catalyst. It consists of roughly spherical particles, ~0.6 mm in diameter. The exact composition and chemical nature are not disclosed but the material has a ratio favoring the AC over the catalyst.

### 3.2. Characterization

The surface composition of the materials was investigated through energy-dispersive X-ray (EDX) spectroscopy, using a Quanta 3D FEG scanning electron microscope (SEM) equipped with EDX detectors. SEM images of the materials were also taken with this instrument at $1 \times 10^{-5}$ mbar. The specific surface areas (SAs) and average pore diameters were recorded with a Quantochrome Autosorb-1 Surface Area and Pore Size Analyser, using nitrogen adsorption–desorption isotherms at 77 K in a relative pressure range of 0.05–0.99 [62]. Surface area was calculated using the Brunauer, Emmett and Teller (BET) equation, as well as the Barrett, Joyner and Halenda (BJH) model and a nonlocal density functional theory (NLDFT) model designed for microporous AC, depending on the material; the results are shown in Table S7 [63,64].

### 3.3. Experimental Setup and Procedure

Two experimental setups were used in the study: a column for single-pass removal measurements and a 1 m$^3$ chamber (described below) for chamber removal tests. The experiments were designed to mimic realistic environmental conditions for a filter used in a PCD targeting ambient air pollution. They took place at room temperature (18–23 °C) and at a set relative humidity (RH) of 50 ± 5%.

For HCHO measurement, both a PTR-MS and CRDS were used; these were the Ionicon PTR-TOF 8000 and the Picarro G2307 Formaldehyde Concentration Analyzer. For the measurement of $NO_2$, a chemiluminescence $NO_x$ analyzer, a Model 42i ($NO-NO_2-NO_x$) Analyser, from Thermo-Fisher Scientific, and a direct absorbance analyzer, a Model 405 nm $NO_2/NO/NO_x$ Monitor, from 2B Technologies, were used. Instrument calibration is described in the Supplementary Materials (SM).

Before testing, the commercial materials were removed from their mounting in order to test all materials under similar physical conditions, except for samples CIF_1, CCF_1, CCF_2 and M_CAT_4, which could not be removed without destroying the active material as they were permanently fixed to a polymer support. When testing, exposure was normalized by the volume of filter material to allow comparison of a diverse range of materials.

#### 3.3.1. Single-Pass

Inlet concentrations of 80–500 ppb HCHO and 50-300 ppb $NO_2$, at face velocities of 0.45 to 0.55 m s$^{-1}$, were introduced to the materials in the single-pass setup. HVAC systems and more powerful portable PCDs use air velocities in this range.

When used for HCHO experiments, the single-pass setup (schematic in Figure S1, with example data in Figure S4) consisted of three lines (6 mm diameter, Teflon), one each for dry air, humid air and HCHO, which then joined to give the bulk flow. The HCHO line consisted of dry air which passed through a heated bubbler (39 °C), containing paraformaldehyde (Merck, extra pure). Each flow was controlled by a Brooks SLA5800 series mass flow controller (MFC) operated by a Brooks 0154 MFC controller and joined in a stainless steel column (25 mm diameter) for mixing before flowing to the test column. Once joined, the bulk flow was 6.2 L min$^{-1}$. The relative flow from each line was adjusted to provide the required HCHO concentration and RH.

The mixing column contained ports for a LS control ES 991 RH probe and a Labjack EI1034 temperature probe. The test column was 16 mm in diameter and contained a mesh for mounting filter materials. Sample ports for the HCHO analyzers were attached before and after the filter and, during experiments, the sampling was alternated between these points at regular intervals. Granular samples

were supported on the mesh and pleated materials were clamped onto it; samples of mass 0.13 g to 2 g were tested. A mesh was also inserted above the materials to ensure that they were not lifted by the air flow.

For $NO_2$ removal experiments, the same setup was used, with a 50.9 ppm $NO_2$ in $N_2$ bottle as the pollutant source rather than paraformaldehyde. A Thermo 42i $NO_x$ monitor was used to measure $NO_x$ concentrations.

### 3.3.2. Chamber

A sealed 1 $m^3$ chamber, consisting of an aluminum frame with stainless steel and Perspex panels was used for chamber removal tests; a schematic is shown in Figure S2 and example data in Figure S6. The chamber contained a mixing fan and a fan driven filter housing to hold filter materials, as well as ports for dry air, humid air, pollutant introduction and pollutant sampling. RH and temperature were measured using the probes described in the single pass experiments.

For each experiment, 10 g of sample was installed in the filter housing before sealing the chamber. The RH was adjusted to the required level before the HCHO was introduced to the chamber. The system was then left, with the analyzer sampling for 15 min to obtain the background decay rate of the chamber. HCHO was introduced by packing a capillary tube with paraformaldehyde, introducing the open end into the chamber and heating the tube. The filter unit was then switched on and HCHO concentration monitored for at least a further 30 min. After the experiment was completed, the data were analyzed by subtracting background removal and fitting the removal curve. The rates of decay or pollutant lifetime in the chamber could then be extracted.

When combined HCHO and $NO_2$ experiments were conducted, the same procedure was followed and, in addition, $NO_2$ was introduced via an MFC (MKS GE50A), and a 2B Technologies Model 405 $NO_x$ monitor was used for detection.

### 3.4. Material Effectiveness

The effectiveness of the materials for pollutant removal was calculated using different metrics for the different experimental setups. For single-pass experiments, removal efficiency (RE) values were calculated according to Equation (1):

$$r = (1 - C_o/C_I)100 \tag{1}$$

where $C_I$ is inlet concentration and $C_o$ is outlet concentration, meaning that the RE value ($r$) accounts for the percentage of the inlet pollutant that is removed by the filter material. This is plotted against, or quoted for, a specific exposure in terms of µg of HCHO per $cm^3$ of filter material.

For the chamber experiments, the background and filter induced removal curves were fitted to first-order exponential decay functions. The background removal rate of the chamber was subtracted from the calculated removal rate with the fan active and the resulting lifetimes compared. The first-order rate constants ($k$) for this decay are used for comparison. Data analysis was performed in RStudio.

## 4. Conclusions

From these results, it is clear that one material, AC_COMP_2, is viable for use in a combined $NO_2$ and HCHO filter. The fact that the composite material is as effective under co-exposure as in separate tests for each one individually demonstrates that the different surfaces of the material are selective for their individual pollutant and will not strongly adsorb or react with the other. In fact, it is essential to the material's effective operation that the AC surface reversibly binds HCHO for release to the catalyst and only chemisorbs the $NO_2$. Equally, the catalyst must only react with HCHO and not be poisoned by $NO_2$ exposure. This material demonstrates an effective new approach to combined HCHO and $NO_2$ removal in a single filter, which is not prohibitively expensive. Therefore, this type of composite filter shows great potential for use in a PCD for indoor environments. The uptake of this material will depend on further testing of its longevity and performance against a more extensive

mix of co-pollutants. Both the (recently released) supported gold nanocluster catalyst CAT_2 and MnO$_2$-based catalyst M_CAT_4 seemed to perform better than HCHO removal catalysts of this type, under ambient conditions, previously reported in the literature and therefore they could be of use in the optimization of PCDs that specifically target HCHO.

## References

1. Household Air Pollution and Health. Available online: https://www.who.int/news-room/fact-sheets/detail/household-air-pollution-and-health (accessed on 11 August 2019).

2. Lelieveld, J.; Pozzer, A.; Pöschl, U.; Fnais, M.; Haines, A.; Münzel, T. Loss of life expectancy from air pollution compared to other risk factors: A worldwide perspective. *Cardiovasc. Res.* **2020**. [CrossRef]

3. Hodgson, A.; Beal, D.; McIlvaine, J.E.R. Sources of formaldehyde, other aldehydes and terpenes in a new manufactured house. *Indoor Air* **2002**, *12*, 235–242. [CrossRef] [PubMed]

4. McDonald, B.C.; De Gouw, J.; Gilman, J.B.; Jathar, S.H.; Akherati, A.; Cappa, C.D.; Jimenez, J.L.; Lee-Taylor, J.; Hayes, P.L.; McKeen, S.A.; et al. Volatile chemical products emerging as largest petrochemical source of urban organic emissions. *Science* **2018**, *359*, 760–764. [CrossRef] [PubMed]

5. Salthammer, T.; Mentese, S.; Marutzky, R. Formaldehyde in the indoor environment. *Chem. Rev.* **2010**, *110*, 2536–2572. [CrossRef] [PubMed]

6. Chen, C.; Zhao, Y.; Zhao, B. Emission rates of multiple air pollutants generated from Chinese residential cooking. *Environ. Sci. Technol.* **2018**, *52*, 1081–1087. [CrossRef] [PubMed]

7. Spiru, P.; Simona, P.L. A review on interactions between energy performance of the buildings, outdoor air pollution and the indoor air quality. *Energy Procedia* **2017**, *128*, 179–186. [CrossRef]

8. Yoshida, T.; Matsunaga, I. A case study on identification of airborne organic compounds and time courses of their concentrations in the cabin of a new car for private use. *Environ. Int.* **2006**, *32*, 58–79. [CrossRef]

9. Yoshida, T.; Matsunaga, I.; Tomioka, K.; Kumagai, S. Interior air pollution in automotive cabins by volatile organic compounds diffusing from interior materials: II. Influence of manufacturer, specifications and usage status on air pollution, and estimation of air pollution levels in initial phases of delivery as a new car. *Indoor Built Environ.* **2006**, *15*, 445–462. [CrossRef]

10. Schupp, T.; Bolt, H.; Hengstler, J.G. Maximum exposure levels for xylene, formaldehyde and acetaldehyde in cars. *Toxicology* **2005**, *206*, 461–470. [CrossRef]

11. Zhang, G.-S.; Li, T.; Luo, M.; Liu, J.-F.; Liu, Z.-R.; Bai, Y.-H. Air pollution in the microenvironment of parked new cars. *Build. Environ.* **2008**, *43*, 315–319. [CrossRef]

12. Huang, S.; Wei, W.; Weschler, L.B.; Salthammer, T.; Kan, H.; Bu, Z.; Zhang, Y. Indoor formaldehyde concentrations in urban China: Preliminary study of some important influencing factors. *Sci. Total. Environ.* **2017**, *590*, 394–405. [CrossRef]

13. Salthammer, T. Formaldehyde in the ambient atmosphere: From an indoor pollutant to an outdoor pollutant? *Angew. Chem. Int. Ed.* **2013**, *52*, 3320–3327. [CrossRef]

14. Nielsen, G.D.; Larsen, S.T.; Wolkoff5P. Re-evaluation of the WHO (2010) formaldehyde indoor air quality guideline for cancer risk assessment. *Arch. Toxicol.* **2016**, *91*, 35–61. [CrossRef] [PubMed]

15. Schwilk, E.; Zhang, L.; Smith, M.T.; Smith, A.H.; Steinmaus, C. Formaldehyde and leukemia: An updated meta-analysis and evaluation of bias. *J. Occup. Environ. Med.* **2010**, *52*, 878–886. [CrossRef] [PubMed]

16. IARC Working Group on the Evaluation of Carcinogenic Risks to Humans Formaldehyde, 2-butoxyethanol and 1-tert-butoxypropan-2-ol. *IARC Monogr Eval Carcinog Risks Hum* **2006**, *88*, 1–478.

17. Zhang, X.; Zhao, Y.; Song, J.; Yang, X.; Zhang, J.; Zhang, Y.; Li, R. differential health effects of constant versus intermittent exposure to formaldehyde in mice: Implications for building ventilation strategies. *Environ. Sci. Technol.* **2018**, *52*, 1551–1560. [CrossRef]

18. IPCC in Climate Change 2013: The Physical Science Basis. *Contribution of Working Group I to the Fifth Assessment Report of the Intergovernmental Panel on Climate Change*; Stocker, T.F., Ed.; Cambridge University Press: New York, NY, USA, 2013.

19. Cofala, J.; Amann, M.; Klimont, Z.; Kupiainen, K.; Höglund-Isaksson, L. Scenarios of global anthropogenic emissions of air pollutants and methane until 2030. *Atmos. Environ.* **2007**, *41*, 8486–8499. [CrossRef]

20. Dennekamp, M.; Howarth, S.; Dick, C.A.J.; Cherrie, J.; Donaldson, K.; Seaton, A. Ultrafine particles and nitrogen oxides generated by gas and electric cooking. *Occup. Environ. Med.* **2001**, *58*, 511–516. [CrossRef]

21. Logue, J.M.; Klepeis, N.E.; Lobscheid, A.B.; Singer, B.C. Pollutant exposures from natural gas cooking burners: A simulation-based assessment for Southern California. *Environ. Heal. Perspect.* **2014**, *122*, 43–50. [CrossRef]

22. Żak, M.; Melaniuk-Wolny, E.; Widziewicz-Rzońca, K. The exposure of pedestrians, drivers and road transport passengers to nitrogen dioxide. *Atmos. Pollut. Res.* **2017**, *8*, 781–790. [CrossRef]

23. Son, B.; Yang, W.; Breysse, P.; Chung, T.; Lee, Y. Estimation of occupational and nonoccupational nitrogen dioxide exposure for Korean taxi drivers using a microenvironmental model. *Environ. Res.* **2004**, *94*, 291–296. [CrossRef]

24. Lewné, M.; Nise, G.; Lind, M.-L.; Gustavsson, P. Exposure to particles and nitrogen dioxide among taxi, bus and lorry drivers. *Int. Arch. Occup. Environ. Heal.* **2005**, *79*, 220–226. [CrossRef] [PubMed]

25. Samoli, E.; Aga, E.; Touloumi, G.; Nisiotis, K.; Forsberg, B.; Lefranc, A.; Pekkanen, J.; Wojtyniak, B.; Schindler, C.; Niciu, E.; et al. Short-term effects of nitrogen dioxide on mortality: An analysis within the APHEA project. *Eur. Respir. J.* **2006**, *27*, 1129–1138. [CrossRef] [PubMed]

26. *WHO Air Quality Guidelines: Global Update 2005: Particulate Matter, Ozone, Nitrogen Dioxide, and Sulfur Dioxide*; World Health Organization: Copenhagen, Denmark, 2006; ISBN 92-890-2192-6.

27. Bernabe, D.; Herrera, R.A.S.; Doma, B.; Fu, M.-L.; Dong, Y.; Wang, Y.-F. Adsorption of low concentration formaldehyde in air using ethylene-diamine-modified diatomaceous earth. *Aerosol Air Qual. Res.* **2015**, *15*, 1652–1661. [CrossRef]

28. Pei, J.; Zhang, J.S. Critical review of catalytic oxidization and chemisorption methods for indoor formaldehyde removal. *Hvac&R Res.* **2011**, *17*, 476–503.

29. Peng, J.; Wang, S. Performance and characterization of supported metal catalysts for complete oxidation of formaldehyde at low temperatures. *Appl. Catal. B Environ.* **2007**, *73*, 282–291. [CrossRef]

30. Na, C.-J.; Yoo, M.-J.; Tsang, D.C.; Kim, H.W.; Kim, K.-H. High-performance materials for effective sorptive removal of formaldehyde in air. *J. Hazard. Mater.* **2019**, *366*, 452–465. [CrossRef]

31. Pei, J.; Zhang, J.S. On the performance and mechanisms of formaldehyde removal by chemi-sorbents. *Chem. Eng. J.* **2011**, *167*, 59–66. [CrossRef]

32. Wang, Q.; Zhong, Z. (Eds.) Functional catalysts for catalytic removal of formaldehyde from air. In *Environmental Functional Nanomaterials*; De Gruyter: Berlin, Germany, 2019; pp. 89–126, ISBN 978-3-11-054418-3.

33. Gandolfo, A.; Marque, S.; Temime-Roussel, B.; Gemayel, R.; Wortham, H.; Truffier-Boutry, D.; Bartolomei, V.; Gligorovski, S. Unexpectedly high levels of organic compounds released by indoor photocatalytic paints. *Environ. Sci. Technol.* **2018**, *52*, 11328–11337. [CrossRef]

34.  Sidheswaran, M.; Chen, W.; Chang, A.; Miller, R.; Cohn, S.; Sullivan, D.; Fisk, W.J.; Kumagai, K.; Destaillats, H. Formaldehyde emissions from ventilation filters under different relative humidity conditions. *Environ. Sci. Technol.* **2013**, *47*, 5336–5343. [CrossRef]

35.  Jeguirim, M.; Belhachemi, M.; Limousy, L.; Bennici, S. Adsorption/reduction of nitrogen dioxide on activated carbons: Textural properties versus surface chemistry–A review. *Chem. Eng. J.* **2018**, *347*, 493–504. [CrossRef]

36.  Chen, C.; Li, J.; Tan, X.; Wang, X. Comparative study of graphene oxide, activated carbon and carbon nanotubes as adsorbents for copper decontamination. *Dalton Trans.* **2013**, *42*, 5266. [CrossRef]

37.  Rong, H.; Liu, Z.; Wu, Q.; Pan, D.; Zheng, J. Formaldehyde removal by Rayon-based activated carbon fibers modified by P-aminobenzoic acid. *Cellulose* **2009**, *17*, 205–214. [CrossRef]

38.  Ma, C.; Li, X.; Zhu, T. Removal of low-concentration formaldehyde in air by adsorption on activated carbon modified by hexamethylene diamine. *Carbon* **2011**, *49*, 2873–2875. [CrossRef]

39.  Dunne, E.; Galbally, I.E.; Cheng, M.; Selleck, P.; Molloy, S.B.; Lawson, S.J. Comparison of VOC measurements made by PTR-MS, adsorbent tubes–GC-FID-MS and DNPH derivatization–HPLC during the Sydney Particle Study, 2012: A contribution to the assessment of uncertainty in routine atmospheric VOC measurements. *Atmos. Meas. Tech.* **2018**, *11*, 141–159. [CrossRef]

40.  Cui, L.; Zhang, Z.; Huang, Y.; Lee, S.; Blake, D.R.; Ho, K.F.; Wang, B.; Gao, Y.; Wang, X.; Louie, P.K.K. Measuring OVOCs and VOCs by PTR-MS in an urban roadside microenvironment of Hong Kong: Relative humidity and temperature dependence, and field intercomparisons. *Atmos. Meas. Tech.* **2016**, *9*, 5763–5779. [CrossRef]

41.  Yoo, J.Y.; Park, C.J.; Kim, K.Y.; Son, Y.-S.; Kang, C.-M.; Wolfson, J.M.; Jung, I.-H.; Lee, S.-J.; Koutrakis, P. Development of an activated carbon filter to remove NO 2 and HONO in indoor air. *J. Hazard. Mater.* **2015**, *289*, 184–189. [CrossRef]

42.  Henning, K.-D.; Schäfer, S. Impregnated activated carbon for environmental protection. *Gas Sep. Purif.* **1993**, *7*, 235–240. [CrossRef]

43.  Xu, Q.; Lei, W.; Li, X.; Qi, X.; Yu, J.; Liu, G.; Wang, J.; Zhang, P. Efficient removal of formaldehyde by nanosized gold on well-defined CeO2 nanorods at room temperature. *Environ. Sci. Technol.* **2014**, *48*, 9702–9708. [CrossRef]

44.  Liu, B.; Li, C.; Zhang, Y.; Liu, Y.; Hu, W.; Wang, Q.; Han, L.; Zhang, J. Investigation of catalytic mechanism of formaldehyde oxidation over three-dimensionally ordered macroporous Au/CeO2 catalyst. *Appl. Catal. B Environ.* **2012**, *111*, 467–475. [CrossRef]

45.  Li, H.-F.; Zhang, N.; Chen, P.; Luo, M.-F.; Lu, J.-Q. High surface area Au/CeO2 catalysts for low temperature formaldehyde oxidation. *Appl. Catal. B Environ.* **2011**, *110*, 279–285. [CrossRef]

46.  Jia, M.; Shen, Y.; Li, C.; Bao, Z.; Sheng, S. Effect of supports on the gold catalyst activity for catalytic combustion of CO and HCHO. *Catal. Lett.* **2005**, *99*, 235–239. [CrossRef]

47.  Suresh, S.; Bandosz, T.J. Removal of formaldehyde on carbon based materials: A review of the recent approaches and findings. *Carbon* **2018**, *137*, 207–221. [CrossRef]

48.  Sidheswaran, M.A.; Destaillats, H.; Sullivan, D.P.; Larsen, J.; Fisk, W.J. Quantitative room-temperature mineralization of airborne formaldehyde using manganese oxide catalysts. *Appl. Catal. B Environ.* **2011**, *107*, 34–41. [CrossRef]

49.  Sekine, Y. Oxidative decomposition of formaldehyde by metal oxides at room temperature. *Atmos. Environ.* **2002**, *36*, 5543–5547. [CrossRef]

50.  Liu, F.; Cao, R.; Rong, S.; Zhang, P. Tungsten doped manganese dioxide for efficient removal of gaseous formaldehyde at ambient temperatures. *Mater. Des.* **2018**, *149*, 165–172. [CrossRef]

51.  Li, J.-J.; Yu, E.-Q.; Cai, S.-C.; Chen, X.; Chen, J.; Jia, H.; Xu, Y.-J. Noble metal free, CeO2/LaMnO3 hybrid achieving efficient photo-thermal catalytic decomposition of volatile organic compounds under IR light. *Appl. Catal. B Environ.* **2019**, *240*, 141–152. [CrossRef]

52.  Scirè, S.; Fiorenza, R.; Gulino, A.; Cristaldi, A.; Riccobene, P.M. Selective oxidation of CO in H2-rich stream over ZSM5 zeolites supported Ru catalysts: An investigation on the role of the support and the Ru particle size. *Appl. Catal. A Gen.* **2016**, *520*, 82–91. [CrossRef]

53.  Genty, E.; Brunet, J.; Poupin, C.; Casale, S.; Capelle, S.; Massiani, P.; Siffert, S.; Cousin, R. Co-Al mixed oxides prepared via LDH route using microwaves or ultrasound: Application for catalytic toluene total oxidation. *Catalysts* **2015**, *5*, 851–867. [CrossRef]

54. Han, K.H.; Zhang, J.S.; Guo, B. Toward effective design and adoption of catalyst-based filter for indoor hazards: Formaldehyde abatement under realistic conditions. *J. Hazard. Mater.* **2017**, *331*, 161–170. [CrossRef]

55. Rengga, W.D.P.; Sudibandriyo, M.; Nasikin, M. Adsorptive removal of formaldehyde by chemically bamboo activated carbon with addition of Ag nanoparticle: Equilibrium and kinetic. *MATEC Web Conf.* **2016**, *59*, 4004. [CrossRef]

56. Gorzkowska-Sobas, A.A.; Bjørgo, K.M. *Adsorption Performance of Activated Carbon Towards Toxic Industrial Chemicals*; Norwegian Defence Research Establishment (FFI): Kjeller, Norway, 2015; p. 59.

57. Cortés-Arriagada, D.; Villegas-Escobar, N.; Miranda-Rojas, S.; Toro-Labbé, A. Adsorption/desorption process of formaldehyde onto iron doped graphene: A theoretical exploration from density functional theory calculations. *Phys. Chem. Chem. Phys.* **2017**, *19*, 4179–4189. [CrossRef]

58. Hummers, W.S.; Offeman, R.E. Preparation of graphitic oxide. *J. Am. Chem. Soc.* **1958**, *80*, 1339. [CrossRef]

59. Baur, G.B.; Spring, J.; Kiwi-Minsker, L. Amine functionalized activated carbon fibers as effective structured adsorbents for formaldehyde removal. *Adsorption* **2018**, *24*, 725–732. [CrossRef]

60. Deliyanni, E.; Bandosz, T.J. Effect of carbon surface modification with dimethylamine on reactive adsorption of NOx. *Langmuir* **2011**, *27*, 1837–1843. [CrossRef]

61. Peterson, G.W.; Mahle, J.J.; Decoste, J.B.; Gordon, W.O.; Rossin, J.A. Extraordinary NO2 Removal by the metal-organic framework UiO-66-NH2. *Angew. Chem. Int. Ed.* **2016**, *55*, 6235–6238. [CrossRef]

62. Schultz, L.; Andersson, M.P.; Dalby, K.N.; Müter, D.; Okhrimenko, D.V.; Fordsmand, H.; Stipp, S.L.S. High surface area calcite. *J. Cryst. Growth* **2013**, *371*, 34–38. [CrossRef]

63. Brunauer, S.; Emmett, P.H.; Teller, E. Adsorption of gases in multimolecular layers. *J. Am. Chem. Soc.* **1938**, *60*, 309–319. [CrossRef]

64. Barrett, E.P.; Joyner, L.G.; Halenda, P.P. The determination of pore volume and area distributions in porous substances. I. Computations from nitrogen isotherms. *J. Am. Chem. Soc.* **1951**, *73*, 373–380. [CrossRef]